# Photoinduced electron transfer and geminate recombination in liquids: Analytical theory and Monte Carlo simulations

S. F. Swallen and M. D. Fayer
*Department of Chemistry Stanford University, Stanford, California 94305*

(Received 31 May 1995; accepted 22 August 1995)

Photoinduced electron transfer and geminate recombination in liquid solution are addressed with analytical theory and Monte Carlo simulations. The time-dependent probabilities of the donor being excited and of an ion pair existing are obtained for a system of a donor and many acceptors undergoing diffusive motion. Multiparticle simulations are modeled as a Markov chain and are shown to agree with the analytical formalism presented previously. The calculations are performed using both a simple exponential form of the distance dependence of the transfer rate and using the more general Marcus distance-dependent transfer rate. For a static donor, in the absence of acceptor–acceptor excluded volume, theory and simulations provide identical results, confirming the accuracy of the analytical method. For the calculation of properties of real systems in which both the donor and acceptors diffuse, to make the mathematics tractable, the donor is held static and each acceptor is given a Fick diffusion constant equal to the sum of the diffusion constants of the donor and acceptor, $D=D_d+D_a$. The validity of this approximation is examined in the absence of acceptor–acceptor excluded volume and found to work extremely well under all conditions. It is also examined with acceptor–acceptor excluded volume. In this case, the static donor approximation is found to work generally well up to moderately high acceptor concentrations, $<5\%$ packing fraction. However, the results suggest that at even higher packing fractions, the static donor approximation loses its validity. © *1995 American Institute of Physics.*

## I. INTRODUCTION

Photoinduced electron transfer and geminate recombination (back electron transfer) in liquid solutions is a complex problem that is receiving a great deal of experimental and theoretical attention. The dynamics of electron transfer followed by possible geminate recombination involve a complex interplay of distance-dependent processes and time scales. A donor surrounded by many acceptors can transfer an electron to any of the neighboring molecules, with a probability determined by the distance-dependent transfer rate. Once the electron is transferred, back transfer to the original donor may occur. In liquid solution, the donors and acceptors are constantly moving, changing the spatial arrangements of acceptors about a donor. Electron transfer is a throughspace phenomenon that does not occur only upon contact between a donor and an acceptor. Therefore, to describe the dynamics, it is necessary to keep track of the time-dependent positions of molecules, and to follow the flow of probability as the local configuration evolves in time. An ensemble average must then be performed to calculate experimental observables.

If a donor undergoes electron transfer, it will not fluoresce, so forward electron transfer can be examined by measuring time-resolved donor fluorescence. This gives the probability that the initially excited donor is still excited at some later time. (Without loss of generality, we will take the donors and acceptors to be initially neutral. Forward electron transfer creates a donor cation and an acceptor anion. Geminate recombination recreates neutral ground state donors and acceptors.) Geminate recombination can be studied by measuring the transient absorption of, e.g., the donor cation. The cation absorption grows in with forward electron transfer and decays by geminate recombination. If a donor has acceptors nearby, forward transfer will be fast and geminate recombination can occur prior to forward transfer by another donor that only has access to more distant acceptors. Thus, the time-dependent cation absorption involves overlapping processes of forward transfer and geminate recombination. Despite this increased complexity, the geminate recombination dynamics can be extracted from the ion transient absorption by employing the known forward dynamics, which are independently determined by the time resolved fluorescence measurement.

The overall time-dependent dynamics will be controlled by the distance-dependent forward transfer and back transfer rates and the diffusion constants of the donor and acceptor. Since forward transfer occurs between neutral species and back transfer occurs between ions, the distance-dependent forward and back transfer rates will not be the same. Once the ions are formed, the ions will be attracted to each other, enhancing the probability of geminate recombination. It is possible for the ions to escape and go on to do useful chemistry. A proper theoretical analysis will be able to describe the dynamics and potentially extract the distance dependence of the forward and back transfer rates from analysis of the experimental data.

Many approaches for modeling photoinduced electron transfer between spatially separated reactants have been proposed in recent years.[1–16] These methods have varying degrees of complexity. For solid isotropic solutions (no diffusion), many important issues have been addressed in detail. In solid solution, the problem of distance-dependent forward transfer has been treated theoretically,[17–22] and experimental data can be modeled well.[23–27] In addition, an exact statistical mechanical treatment of back transfer (geminate recom-

 0021-9606/95/103(20)/8864/9/$6.00 

bination) has been developed and used to fit data.[23,28] However, the problem becomes much more complex in liquid solutions since diffusion of the donors and acceptors must be included. A treatment of photoinduced electron transfer with geminate recombination including diffusion and Coulomb interaction between the ions has been presented.[29,30] Initially inspired by the Smoluchowski and Collins and Kimball approaches, this latter method includes a full treatment of throughspace distance-dependent electron transfer probabilities.

It is notable, however, that a significant approximation has been made concerning the diffusion constants of donors and acceptors. When solving for the time-dependent forward and back transfer probabilities, an accurate description of the rates of approach of the donor and acceptor species is important. The diffusion constants for each molecular species in solution can be measured, and individual particle motions can be modeled. However, the correlated motions for members of a systems of particles, such as a donor and a surrounding distribution of acceptors, is more difficult to include fully. As a mathematical simplification, it has been suggested that isotropic diffusion be modeled with a stationary donor and independently diffusing acceptors.[7,31–33] The acceptors move at a rate equal to the sum of the donor and acceptor individual rates. In this approximation, the acceptors undergo diffusive motion characterized by a Fick diffusion constant equal to $D=D_d+D_a$, i.e., a diffusion constant that is the sum of the donor and acceptor diffusion constants. In essence, this assumes that the donor molecule is infinitely massive and does not move, while the rate of diffusion of each acceptor is increased correspondingly.

In the low concentration limit, in which only one acceptor interacts with the photoexcited donor, this is exact. It amounts to a coordinate transformation. However, when there is more than one acceptor, the motions are correlated. In a reference frame centered on the donor, a motion by the donor in one direction is rigorously represented by a concerted motion of all the other particles in the opposite direction. Conversely, in a model in which the donor is fixed, and the acceptors move with $D=D_d+D_a$, the acceptors no longer display correlated motion. Noyes has discussed this issue at some length,[33] though he is inconclusive in his assessment of the problem. He postulates that for point particles, this approximation is probably valid, given the ''relatively'' uncorrelated nature of each particles' movement. This is not an obvious conclusion. In the reference frame of a static donor, the vector of motion for each acceptor has two sources. The first is the standard random motion of particles in solution. This motion is unique and independent for each acceptor. The second contribution to the acceptor diffusion is due to the donor. This value is equal in direction and magnitude for every acceptor. In this way, the motions of all particles are fundamentally correlated. This is true even for point particles.

In this paper we compare theoretical calculations with Monte Carlo simulations of photoinduced electron transfer and geminate recombination in liquid solution in which the donors and acceptors are diffusing. A formal solution has been developed that describes the probability of a photoexcited donor remaining excited at time $t$, $\langle P_{ex}(t)\rangle$, and the probability of a donor–acceptor ion pair existing at time $t$, $\langle P_{ct}(t)\rangle$.[29,30,34] These quantities are related to the experimental observables of time-resolved fluorescence of the donor and ion transient absorption as discussed above. Previous comparison of the analytical formalism to Monte Carlo simulation for solid solutions (no diffusion) has demonstrated the mathematical accuracy of this analytical formalism.[35] In this paper, the simulations are extended to liquid solutions in which molecular diffusion is occurring. There are two purposes for performing these calculations. The first is to conclusively verify the validity of the analytical formalism with diffusion as well as to ensure that the simulations have been accurately implemented. This is done for an infinitely massive donor, i.e., no donor diffusion. This permits the accuracy of the analytical theory to be tested in the absence of the $D=D_d+D_a$ approximation. The second purpose is to examine the effects of the static donor approximation, i.e., a system in which both the donor and acceptors are diffusing can be approximated by a fixed donor and acceptors with diffusion constant, $D=D_d+D_a$. The accuracy of this assumption, in the context of the electron transfer problem, is very important. Mathematically describing diffusive motion in this way makes possible the analytic solution of the problem, yielding explicit expressions for electron transfer probabilities in liquid solution. Agreement between the simulations and the theory with the approximation validates the analytical method and emphasizes the latter's applicability to understanding the dynamics of electron transfer in solution and analyzing experimental results.

The model that is examined theoretically is a three level system that is applicable in many, but not all, experimental situations. The lowest level (ground state) is a neutral ground state donor and neutral acceptors. The highest level is an electronically excited donor (excited at time $t=0$) and neutral acceptors. The third level is an unexcited donor cation and one acceptor anion with the rest of the acceptors remaining neutral. Forward electron transfer can take place from the excited donor to any acceptor. However, back electron transfer is taken to be geminate. Back transfer can occur only from the anion that initially receives the electron. Transfer of the electron to another donor cation is not possible because of the low concentration of donors. Electron transfer from the acceptor anion to another neutral acceptor is not included in the treatment, although this is physically possible. The exclusion of electron hopping from one acceptor to another has a physical basis. The geminate recombination path of back transfer to the donor cation is energetically downhill, i.e., there is a driving force. This is not the case for acceptor-to-acceptor transfer. In the language of the Marcus model,[9,36] if the back transfer is in the normal region or the mildly inverted region, the barrier for geminate recombination will generally be small compared to the barrier for acceptor–acceptor electron hopping. In the highly inverted regime, semiclassical theory,[37] which replaces Marcus theory, shows that the transfer rate does not become increasingly slow, as predicted by Marcus theory. Furthermore, forward electron transfer is relatively short range, occurring over only a few angstroms of donor–acceptor separation. Even for solutions

with a very high concentration of acceptors (a few tenths molar), the separation between the cation and anion is small compared to the average acceptor–acceptor separation. This also adds to the high probability that recombination will be geminate. Therefore, the three level model treated here, which does not include acceptor–acceptor electron hopping, will be applicable to many real experimental systems, and proper treatment of this model is a precursor to the inclusion of other effects like electron hopping between acceptors.

## II. ANALYTICAL SOLUTIONS

The model under consideration is the three level system, composed of a photoexcited donor with neutral ground state acceptors (D*A), an ion pair formed by forward transfer ($D^+A^-$), and a ground state neutral pair (DA) created by geminate recombination. The distance-dependent rate constants for forward and back electron transfer are given by $k_f(R)$ and $k_b(R)$, respectively, and the fluorescence lifetime of the excited donor in the absence of electron transfer is $\tau$. As discussed above, back transfer is geminate. It is possible for the ion pair to separate to form long-lived radical ions. This will be discussed following the presentation of the results.

The partial differential equations describing electron transfer in a system of one donor and one acceptor with diffusion are, for the survival probability of the excited state,

$$\frac{\partial}{\partial t} S_{\mathrm{ex}}(R,t|R_0) = D\ \nabla^2 S_{\mathrm{ex}}(R,t|R_0) - k_f(R) S_{\mathrm{ex}}(R,t|R_0), \tag{1}$$

and for the ion pair (charge transfer) state:

$$\frac{\partial}{\partial t} S_{\mathrm{ct}}(R,t|R_0) = L_R S_{\mathrm{ct}}(R,t|R_0) - k_b(R) S_{\mathrm{ct}}(R,t|R_0), \tag{2}$$

where $R_0$ is the initial position of the acceptor at time $t=0$ and $R$ is the position at a time $t$ later. For a spherically symmetric system, the diffusional operator $\nabla^2$ is defined as

$$\nabla_R^2 = \frac{2}{R}\frac{\partial}{\partial R} + \frac{\partial^2}{\partial R^2}, \tag{3}$$

and the Smoluchowski operator $L_R$ is

$$L_R = \frac{D}{R^2}\frac{\partial}{\partial R} R^2 \exp(-V(R))\frac{\partial}{\partial R}\exp(V(R)), \tag{4}$$

where $V(R)$ is the Coulomb potential between the donor cation and acceptor anion. Both Eqs. (1) and (2) are solved with reflecting boundary conditions at the van der Walls contact distance between donor and acceptor. The initial conditions for both the excited donor probability and ion survival probability are 1.

For the general case of one donor surrounded by $N$ acceptors in an initial spatial arrangement given by $\bar{R}_0 = (R_{01}, R_{02}, \ldots, R_{0N})$, and in a position $\bar{R} = (R_1, R_2, \ldots, R_N)$ at a time $t$ later, the excited state probability is

$$\frac{\partial}{\partial t} P_{\mathrm{ex}}(\bar{R},t|\bar{R}_0) = \sum_{j=1}^{N} [D\nabla_j^2 - k_f(R_j)] P_{\mathrm{ex}}(\bar{R},t|\bar{R}_0), \tag{5}$$

and the ion state probability is

$$\frac{\partial}{\partial t} P_{\mathrm{ct}}^i(\bar{R},t|\bar{R}_0) = \sum_{j=1}^{N} L_{R_j} P_{\mathrm{ct}}^i(\bar{R},t|\bar{R}_0) - k_b(R_i) P_{\mathrm{ct}}^i(\bar{R},t|\bar{R}_0) + k_f(R_i) P_{\mathrm{ex}}(\bar{R},t|\bar{R}_0), \quad i=(1,\ldots,N), \tag{6}$$

where $P_{\mathrm{ct}}^i(\bar{R},t|\bar{R}_0)$ is the probability that the system exists as a charge transfer ion pair and the $i$th acceptor has the electron, given that the acceptors started at $\bar{R}_0$ and are in the configuration $\bar{R}$ at time $t$. The solutions to these equations have been derived previously with donor–acceptor excluded volume but without acceptor–acceptor excluded volume.[34] (Acceptor–acceptor excluded volume has also been treated,[30,35] but is only necessary at very high acceptor concentrations.) The result for the excited state probability is

$$\langle P_{\mathrm{ex}}(t)\rangle = \exp(-t/\tau) \times \exp\left(-4\pi C \int_{R_m}^{\infty} [1 - S_{\mathrm{ex}}(R,t)] R^2\, dR\right), \tag{7}$$

where $\exp(-t/\tau)$ accounts for the finite fluorescence lifetime of the excited state and $R_m$ is the donor–acceptor radial contact distance. The ensemble-averaged ion state probability is

$$\langle P_{\mathrm{ct}}(t)\rangle = 4\pi C \int_{R_m}^{\infty}\int_0^t S_{\mathrm{ct}}(R,t-t') k_f(R) S_{\mathrm{ex}}(R,t') \times \langle P_{\mathrm{ex}}(t')\rangle dt'\ R^2\, dR. \tag{8}$$

The one-acceptor survival probabilities $S_{\mathrm{ex}}$ and $S_{\mathrm{ct}}$ are given by numerical solutions to Eqs. (1) and (2), respectively. The state probability functions, Eqs. (7) and (8), are exact solutions in the absence of acceptor–acceptor excluded volume and with the donor diffusion constant $D_d = 0$. Comparisons with Monte Carlo simulations, presented in the next section, will test the validity of these equations and examine the accuracy of the diffusion constant approximation, $D = D_d + D_a$.

The form of the distance-dependent electron transfer rate constants are given by Marcus as[36]

$$k(R) = \frac{2\pi}{\hbar\sqrt{4\pi\lambda k_B T}} J_0^2 \exp\left(\frac{-(\Delta G + \lambda)^2}{4\pi k_B T}\right) \times \exp(-\beta(R - R_m)). \tag{9}$$

$J_0$ is the magnitude of the transfer matrix element at the donor–acceptor contact distance $R_m$. $\Delta G$ is the free energy change associated with the electron transfer reaction. $\beta$ is the attenuation constant of the donor and acceptor wave functions. The solvent reorganization energy $\lambda$ is expressed as

$$\lambda = \frac{e^2}{2}\left(\frac{1}{\epsilon_{\mathrm{op}}} - \frac{1}{\epsilon_s}\right)\left(\frac{1}{R_{\mathrm{don}}} + \frac{1}{R_{\mathrm{acc}}} - \frac{2}{r}\right), \tag{10}$$

where $\epsilon_{\mathrm{op}}$ and $\epsilon_s$ are the optical and static solvent dielectric constants. $R_{\mathrm{don}}$ and $R_{\mathrm{acc}}$ are the van der Walls radii of the donor and acceptor. This form applies to both forward and back transfer, but, in general, the values of the various pa-

rameters will be different for forward and back transfer. The Marcus expression accounts for the significant molecular characteristics that influence electron transfer. Under certain conditions, the functional form of the Marcus expression exhibits an exponential dependence with distance. In this case, one can simplify these expressions by approximating the rate constants for forward and back transfer to be

$$k_f(R)=\frac{1}{\tau}\exp\left(\frac{R_f-R}{a_f}\right),\quad k_b(R)=\frac{1}{\tau}\exp\left(\frac{R_b-R}{a_b}\right). \tag{11}$$

$a_f$ and $a_b$ parametrize the spatial fall-off of the donor and acceptor wave function overlap in forward and back transfer, respectively, while $R_f$ and $R_b$ reflect the distance dependence of each process. Both the Marcus form and the exponential form of the rate constants will be used below in the calculations and the comparisons between theory and simulation.

## III. MARKOV CHAIN REPRESENTATION AND MONTE CARLO SIMULATIONS

Time-dependent electron transfer is a stochastic process that can be modeled as a finite, absorbing Markov chain. This is a process in which the probability of an outcome (transfer or fluorescence) at each time step is dependent only on the outcome of the immediately preceding step, and all states are mutually exclusive.[38–40] The physical constraints of the electron transfer process give rise to a reducible, aperiodic Markov chain, i.e., a period of unity. By discretizing the forward and back transfer events into a series of finite, but small time steps, it is possible to derive the homogeneous transition probability function for each state of the three level system (neutral pair, excited state pair, and ion state pair). In conjunction with the initial ($t=0$) probability function, this can be used to find the probability of being in each state at subsequent time steps. The transition probabilities for all possible events of this system in a unit time step $\Delta t$ are defined by the matrix

| Initial \ Final | Excited | Ion | Ground |
|---|---|---|---|
| Excited | $P_{\mathrm{ex}}$ | $P_f$ | $P_{\mathrm{fl}}$ |
| Ion | 0 | $P_{\mathrm{ct}}$ | $P_b$ |
| Ground | 0 | 0 | 1 |

where the labels identify the three states of the system, and each element is the probability of transfer from one state to another in a single time step. The value of each transition element is given by

$$\begin{aligned}
&\text{(remaining excited)} && P_{\mathrm{ex}}=\mathrm{ex},\\
&\text{(forward transfer)} && P_f=\left(\frac{f}{f+\mathrm{fl}}\right)(1-\mathrm{ex}),\\
&\text{(fluorescence)} && P_{\mathrm{fl}}=\left(\frac{\mathrm{fl}}{f+\mathrm{fl}}\right)(1-\mathrm{ex}),\\
&\text{(remaining as ions)} && P_{\mathrm{ct}}=1-b,\\
&\text{(back transfer)} && P_b=b,
\end{aligned} \tag{12}$$

where the variables ex, $f$, fl, and $b$ are defined as

$$\begin{aligned}
\mathrm{ex}&=\exp\left(\frac{-\Delta t}{\tau}\right)\exp\left(-\sum_{i=1}^{N}k_f(R_i)\Delta t\right),\\
f&=1-\exp\left(-\sum_{i=1}^{N}k_f(R_i)\Delta t\right),\\
\mathrm{fl}&=1-\exp\left(\frac{-\Delta t}{\tau}\right),\\
b&=1-\exp(-k_b(R)\Delta t),
\end{aligned} \tag{13}$$

and the summations are over all $N$ acceptors $i=(1,\ldots,N)$. The value of $N$ is given by the concentration of acceptor molecules and an empirically determined system volume. The latter value is chosen such that all relevant electron transfer events are included. In addition, it was important that the system be large enough that typical diffusive particle motions were unaffected by edge effects of a noninfinite volume.

By expressing the electron transfer process as a finite Markov chain, it is straightforward to solve for the state probabilities by means of Monte Carlo techniques. This is achieved by randomly choosing a microstate of the system (a particular configuration of $N$ acceptors about a donor at the origin), and determining the lifetime of the excited and ion states. The time-dependent probabilities are then determined by ensemble averaging over a sufficient number of microstates. By properly allowing the particles to spatially diffuse at each time step, the Monte Carlo simulations should exactly reproduce the correct analytical solutions given in Eqs. (7) and (8).

The general techniques used in the Monte Carlo simulations have been well covered in the literature.[35,41–44] By choosing sufficiently ''random'' numbers over appropriate ranges, uniform probability distributions were used both for transfer probability determination, as well as diffusive particle motion. Over a large number of time steps, it was important that typical paths of motion for each particle resembled uncorrelated (Brownian) motion. For this reason in particular, it was important to calculate sufficiently small $\Delta t$ time steps. Values of $\Delta t$ were chosen such that the maximum scalar of motion was small on the distance scale of electron transfer. This varied depending on the electron transfer parameters. Typical values ranged from 0.03 to 0.3 Å. In all cases, the step size was reduced until further reduction did not produce significant changes in the results. The system size was chosen to be larger than the radius of significant electron transfer interaction, as well as large enough to minimize edge effects in a noninfinite system. The appropriate volume was determined by expanding the size of the system until no significant changes in the results were caused by a further increase in volume. For the distance-dependent transfer rates and the diffusion constants employed in the calculations presented below, a volume having a radius of 50 Å was sufficiently large. Edge effects were further minimized by using the minimum image convention with periodic

boundary conditions.[41,43] Conditions necessary to create an initial random configuration in such a system have been discussed in detail elsewhere.[35,41,44]

The initial conditions for the excited and ion states are $\langle P_{ex}(t=0)\rangle=1$ and $\langle P_{ct}(t=0)\rangle=0$. At the first time step, all particles were randomly moved a radial distance determined by the chosen Fick diffusion constant $D$. This scalar of motion was calculated from $R_{diff}=\sqrt{6D\,\Delta t}$. Each final particle placement was found by randomly choosing the polar coordinates $\phi$ and $\theta$ from the respective weighted distribution for each degree of freedom.[35,45] Once the new configuration was obtained, the probability of forward transfer, $P_f$, fluorescence, $P_{fl}$, or of remaining in the excited state, $P_{ex}$, was calculated via Eq. (12). A random number was chosen on the set $[0\cdot\cdot1]$, determining which event occurred. When it was found that fluorescence took place, a neutral pair was created, thus entering the absorbing state at the terminus of the Markov chain. Conversely, if forward transfer occurred, it was necessary to determine which acceptor received the electron. The chance of the $i$th particle becoming an anion was $P_i=k_f(R_i)/\Sigma_i k_f(R_i)$, and again a random number was used to make the selection. If the latter event happened (remaining in the excited state), the processes of diffusion and possible transfer were again examined. This was repeated until a transitional event took place.

If at any time forward transfer did occur, then the ion state had to be examined. As this latter state is only a two particle process, the computational effort could, under certain conditions, be substantially reduced to include only the ion pair. This is possible when acceptor–acceptor excluded volume is not included. In this case, the acceptor positions become uncorrelated, and the ion pair is unaffected by the presence of the other N-1 neutral acceptors. This scenario is particularly significant in that it makes the question of donor–acceptor correlated diffusion during back transfer a moot point. On the other hand, if acceptor volume is included, then all particle positions and motions must be retained, even during the ion state calculations. This means that the system is still dependent on all $N+1$ particles, and the validity of the static donor approximation must be examined. In the results presented below, simulations with and without acceptor–acceptor excluded volume are compared. In all cases, donor–acceptor excluded volume is included in the simulations and in the analytical calculations.

In the study of back transfer between an ion pair, diffusive motion may be modified by Coulombic attraction between the newly created oppositely charged ions. To account for this, the likelihood of the ions moving in any given direction is made to be dependent upon the change in potential energy before and after the step. If the new position resulted in a decrease of the potential of the ion pair, the move was accepted. If the potential energy increased, it was accepted with an inverse exponential probability, with respect to the magnitude of change.[41] After each step, the probability of back transfer was determined from Eq. (12). Again, a random number was chosen to determine which event occurred. This either resulted in the creation of the neutral state and termination of the chain, or the ion remained. If the ion still existed, the simulation was continued.

For a given initial configuration, the time bins during which each state was occupied were recorded in separate histograms. By averaging over a sufficient number of unique starting configurations, a time-dependent ensemble average of state probabilities was found. These solutions are directly comparable to the analytical solutions of Eqs. (7) and (8). When the donor is held fixed in both the simulation and analytical models, with no acceptor excluded volume, the two methods are identical formulations of the same physical model. When the donor is allowed to diffuse freely in the simulations, the comparison between methods can examine the validity of fixing the donor and assigning the acceptor a diffusion constant $D=D_d+D_a$.

All the Monte Carlo simulations employed a random number generator to uniformly select values in the range $[0\cdot\cdot1]$. These values were then used to sample the ranges of the functions of interest. The algorithm to select random numbers was developed by Marsaglia and Zaman.[46] This algorithm required 24 input seed numbers, which were obtained from a simpler random number generator with a shorter period.[47] The numerical calculations were done on an IBM RS6000 model 3BT workstation. All programs were written in the *C* language. Several standard subroutines were obtained from algorithms written by Press *et al.*[48]

## IV. RESULTS

The agreement between the analytical theory and the Monte Carlo simulations when the donor is held fixed can be used as a multipurpose check on both methods of analysis. Figure 1 shows $\langle P_{ex}(t)\rangle$ obtained both ways for a variety of electron transfer parameters (given in the figure caption), using both the exponential form and the Marcus form of the rate constant $k_f(R)$. The analytical solutions were obtained directly from Eq. (7), and the simulations were performed keeping the donor fixed and only allowing the acceptors to move. For both methods, donor–acceptor excluded volume, with a radius equal to the van der Walls contact distance of the two molecules, was included, but acceptor–acceptor excluded volume was not. Fluorescence decay was not included so that the role of electron transfer is emphasized. It is clear that in every case the two methods agree. The small differences that appear in the figure arise from convergence criteria in both the analytical calculations and the simulations. The figure shows a small sampling of the large number of calculations that were performed. Agreement is seen for any value of all the system variables, including any set of electron transfer parameters, all particle concentrations, and any form of the forward transfer rate distance dependence. The results emphasize that not only have all the spatial averages been done correctly in the analytical method, but that the Markov chain approach accurately describes the system and has been implemented correctly.

Figure 2 displays the functional form of the rate constants versus radial distance for the calculations in Fig. 1. The magnitudes of each $K_f(R)$ plot in Fig. 2 have been scaled to have a maximum of one for the purposes of comparison. In practice, the absolute magnitudes of the transfer rate constants varied over seven orders of magnitude, depending on the parameters chosen. The transfer parameters

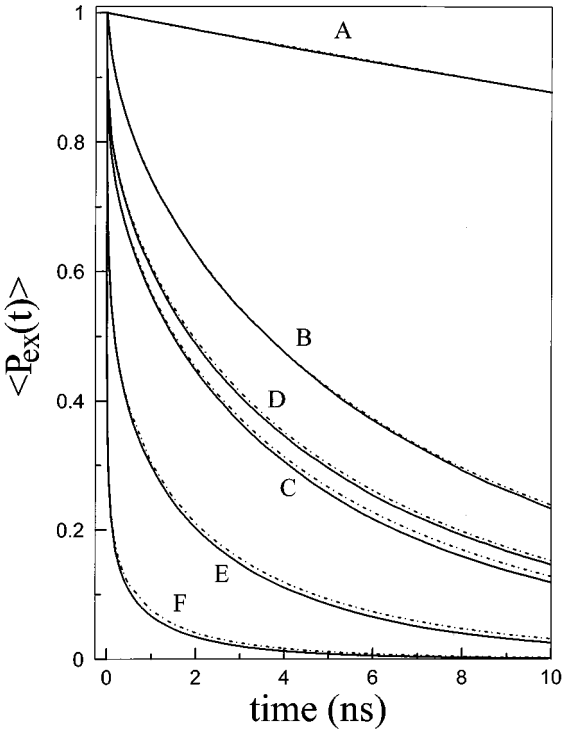


FIG. 1. Comparison of $\langle P_{ex}(t)\rangle$ calculations obtained from analytic solution (solid lines), and from Monte Carlo simulation (dashed lines). Donor–acceptor contact distance $R_m$ is the sum of $R_{don}$=5.4 Å and $R_{acc}$=3.6 Å. Acceptor concentration was $0.1M$, and diffusion constant=10 Å$^2$/ns. Curves A–C were calculated with an exponential form of the electron transfer rate constant [Eq. (12)], with $\tau$=15.0 ns. A, $a_f$=1.0, $R_f$=10.0; B, $a_f$=0.5 $R_f$=12.0; C, $a_f$=0.2, $R_f$=12.0. Curves D–F employed the Marcus form of the rate constant [Eq. (10)]. D, $J_0$=400, $\beta$=3.0, $\Delta G$=−1.0; E, $J_0$=100, $\beta$=1, $\Delta G$=−0.5; F, $J_0$=1000, $\beta$=1, $\Delta G$=−1.2. The value of λ is obtained with $\epsilon_{op}$=2.2, $\epsilon_s$=8.5.

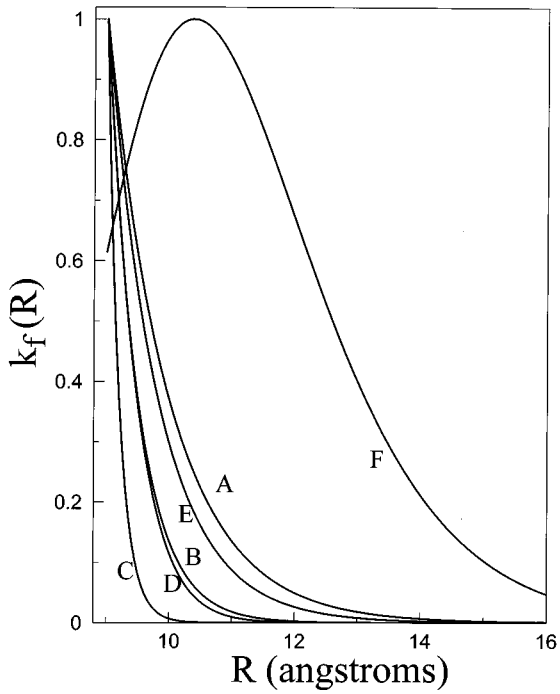


FIG. 2. This figure displays the distance-dependent functional shape for the transfer rate constants used in the calculations of Fig. 1. All curves have been normalized such that the maximum intensity is set to 1, in order to more clearly exhibit the various distance dependences. The absolute magnitudes of these curves actually vary over seven orders of magnitude.

for curves F in Figs. 1 and 2 were chosen to show that analytical theory and the simulations agree even when the distance-dependent transfer rate is not exponentially decaying, or even monotonically decreasing. For all cases, regardless of transfer rate magnitude or functional form, the analytical solution for $\langle P_{ex}(t)\rangle$ agrees exactly with the Monte Carlo simulations. The very slight mismatches on the curves shown in Fig. 1 are the result of computational time constraints limiting the convergence criteria during the calculations. It is important to recognize that both the analytical theory and the simulations involve numerical difficulties in calculating the curves. This is particularly true of $\langle P_{ct}(t)\rangle$ shown below, calculated with the analytical theory. It is possible to obtain numerical solutions of the differential equations that are qualitatively reasonable and that seem to have converged, when in fact, the calculations are far from convergence. There is no firm criteria that can be stated for step sizes in the calculations that will work under all circumstances because the necessary conditions for converges depend on the electron transfer parameters. However, it is important to note that a significant reduction in step sizes is required to test for convergence. Therefore, great care must be exercised if meaningful results are to be obtained.

Comparisons of calculations of $\langle P_{ct}(t)\rangle$ that include forward transfer and geminate recombination obtained from the analytical solution [Eq. (8)] and by simulation [Eq. (12)] are shown in Fig. 3. The donor was held stationary in both the analytic and simulated curves, and fluorescence decay was not included. Donor–acceptor excluded volume was accounted for, but acceptor–acceptor excluded volume was not. A wide variety of transfer parameters, as well as both the Marcus and exponential forms of the distance-dependent transfer rate, were examined. In every case, the two methods of calculating $\langle P_{ct}(t)\rangle$ resulted in essentially perfect agreement. The agreement of the results emphasizes the mathematical accuracy of the analytical statistical mechanical approach presented here (which is described in more detail elsewhere[34]). Figure 3 shows that it is possible to accurately calculate the time-dependent ion concentration, generated by forward transfer and decaying through geminate recombination, in systems with a diffusing donor and acceptors, and diffusing ions that are attracted to each other by a Coulombic interaction. The agreement is perfect within the error caused by convergence criteria for any choice of the forward and back transfer parameters and for either the exponential or Marcus form of the distance dependence of the transfer rate.

The significant advantage of using the analytical theory is the speed with which the time-dependent properties of a system and experimental observables can be calculated. Computer CPU time required to find $\langle P_{ex}(t)\rangle$ and $\langle P_{ct}(t)\rangle$ via Eqs. (7) and (8) is several minutes. In contrast, the Monte Carlo simulations, depending on concentration and parameter values, require a few hours to a few tens of hours. Simulations that include finite acceptor volumes can require many days to reach convergence.

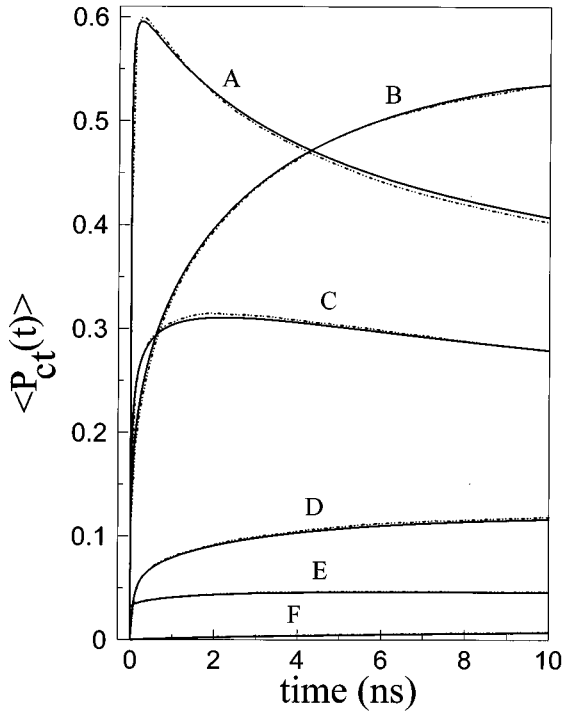


FIG. 3. Comparison of ion state probability $\langle P_{ct}(t)\rangle$ calculations obtained from analytic solution (solid lines) and simulation (dashed lines). Particle sizes and solvent dielectric values are given in Fig. 1. Acceptor concentration was $0.1M$, and diffusion constant=10 Å$^2$/ns. Curves B, D, and F utilized the exponential transfer rate constant [Eq. (12)] with $\tau$=15.0 ns, while curves A, C, and E used the Marcus form [Eq. (10)]. The values for the parameters used in each curve are A, $J_{0f}$=1000, $\beta_f$=1, $\Delta G_f$=−1.2, $J_{0b}$=400, $\beta_b$=3, $\Delta G_b$=−1.0; B, $a_f$=0.2, $R_f$=12, $a_b$=1.0, $R_b$=12; C, $J_{0f}$=100, $\beta_f$=1, $\Delta G_f$=−0.5, $J_{0b}$=400, $\beta_b$=3, $\Delta G_b$=−1.0; D, $a_f$=0.5, $R_f$=12, $a_b$=0.5, $R_b$=12; E, $J_{0f}$=400, $\beta_f$=3, $\Delta G_f$=−1.0, $J_{0b}$=400, $\beta_b$=3, $\Delta G_b$=−1.0; F, $a_f$=1.0, $R_f$=10, $a_b$=0.2, $R_b$=12.

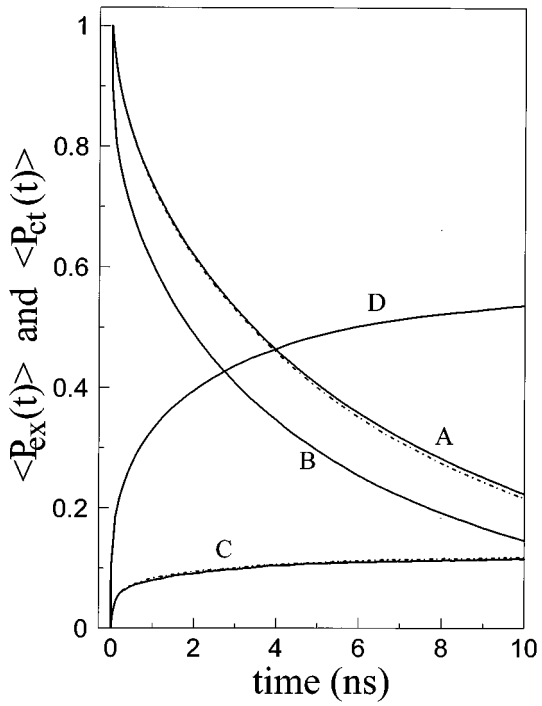


FIG. 4. Comparison of simulations using the static donor approximation with the acceptor diffusion constant $D=D_d+D_a$ (solid lines), with simulations in which the donor and the acceptors undergo diffusion (dashed lines). Contact distance $R_m$=9.0 Å. Acceptor concentration was $0.1M$ and $D_d=D_a$=5.0 Å$^2$/ns. The value of $\tau$=15 ns. Curves A and B are excited state probabilities $\langle P_{ex}(t)\rangle$, with parameters A, $a_f$=0.5, $R_f$=12; B, $a_b$=0.2, $R_b$=12.0. Curves C and D are ion state probabilities $\langle P_{ct}(t)\rangle$, with parameters C, $a_f$=0.5, $R_f$=12, $a_b$=0.5, $R_b$=12; D, $a_f$=0.2, $R_f$=12.0, $a_b$=1.0, $R_b$=10.0. Curves B and D were calculated by both methods, but agree too well to be distinguishable.

In the calculations presented above, acceptor–acceptor excluded volume is not included. Detailed examination of acceptor–acceptor excluded volume in solid solutions[35] shows that it is not important at moderate and low concentrations. It only becomes significant for concentrations above a few tenths molar. An approximate method of handling acceptor–acceptor excluded volume up to higher concentrations has been developed,[35] but this approach fails at very high concentrations. These very high concentrations ($\sim 1M$) are not generally encountered in real experimental systems. More important than acceptor–acceptor excluded volume is the static donor approximation. In the calculations presented above, the donor is fixed in both the theory and simulations. In real systems the donor and acceptors undergo diffusive motion. In the simulations, it is straightforward to have the donor diffuse. In the analytical theory, the donor is always held fixed, and its diffusion is approximated by giving the acceptors a diffusion constant of $D=D_a+D_d$. Making the static donor approximation enables the analytical theory to be applied to real experimental systems, but the analytical theory is useful only if this approximation is accurate.

Figure 4 examines this approximation in the absence of acceptor–acceptor excluded volume. Simulations of $\langle P_{ex}(t)\rangle$ and $\langle P_{ct}(t)\rangle$ with a static donor are compared to those that allow both the donor and acceptors to move freely. In the former case, the acceptors were moved with a diffusion constant equal to the sum of the donor and acceptor diffusion constants. The figure shows that the static donor approximation is nearly flawless. Curves B and D are actually pairs of curves that are indistinguishable in the figure. The displayed calculations are for the exponential form of the distance dependent transfer rate. A large number of calculations were performed using both the exponential [Eq. (11)] and the Marcus [Eq. (9)] forms of the transfer rate. For any choice of transfer parameters, both methods (static or mobile donor) gave results that are, within numerical accuracy, identical. The agreement was unaffected by acceptor concentration, transfer parameters, or diffusion constant. Identical agreement is found regardless of the functional form of the transfer rate. These results confirm the validity of the static donor approximation in which the true acceptor diffusion constant is replaced with $D=D_a+D_d$ in the calculation.

For low and moderate acceptor concentrations (packing fractions of less than a few percent), inclusion of acceptor–acceptor excluded volume does not affect the accuracy of the static donor approximation because acceptor–acceptor excluded volume is insignificant. However, as the acceptor density increases, acceptor interactions become significant and positions become more correlated. This leads to a noticeable source of error when utilizing the static donor approximation. For finite volume particles, a hard sphere potential

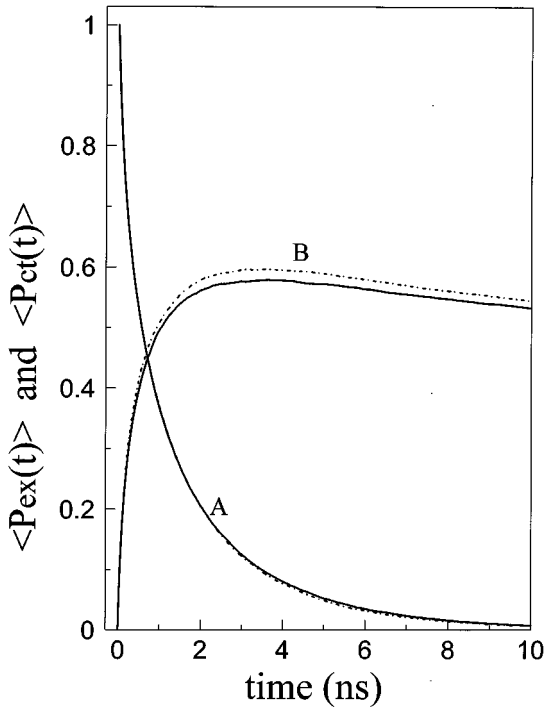


FIG. 5. Comparison of simulations that include acceptor–acceptor excluded volume for the static donor approximation (solid lines) and for the case in which both donor and acceptors are allowed to diffuse (dashed lines). The donors and acceptors were given a finite volume and interact with a hard sphere potential. Donor radius=5.4 Å, acceptor radius=3.6 Å. Acceptor concentration is $0.3M$ (packing fraction=6.7%), diffusion constant $D_d=D_a=5.0$ Å$^2$/ns. The exponential form of the distance-dependent transfer rate was used. Curves A are the excited state probabilities $\langle P_{\rm ex}(t)\rangle$, with parameters $a_f=0.5$, $R_f=12.0$. Curves B are the ion state probabilities $\langle P_{\rm ct}(t)\rangle$, with parameters $a_f=0.5$, $R_f=12.0$, $a_b=1.0$, $R_b=12.0$.

was used for the interaction potential. As seen in Fig. 5, comparison between simulations with a static and a mobile donor are in some disagreement for the ion state calculations. For either $P_{\rm ex}$ or $P_{\rm ct}$, the disparity varied with choice of transfer parameters, diffusion constant, and packing fraction. The example shown in Fig. 5 exhibits the error inherent with an acceptor concentration of $0.3M$ (6.7% packing fraction) in a reasonably viscous medium ($D=10.0$ Å$^2$/ns). At concentrations less than $0.3M$, little error is seen. However, the discrepancies increase significantly with acceptor density and diffusion constant.

## V. CONCLUDING REMARKS

In liquid systems, diffusion can play a significant role in electron transfer and geminate recombination. While significantly increasing the rates of forward and back transfer, diffusion can also lead to a finite population of ion pairs that can survive for a greatly extended length of time. It is possible for the pair to separate, resulting in solvated species that may be useful as sources of chemical energy. It is important for an understanding of these processes to be able to adequately model the energetics and dynamics that occur. The results presented here, comparing Monte Carlo simulations with the previously developed analytical theory, show that for a fixed donor the theory provides an accurate description for an ideal three level system including acceptor diffusion up to moderate acceptor concentrations (acceptor–acceptor excluded volume is relatively unimportant).

Since in real systems the donor undergoes diffusion, the validity of the static donor approximation was tested. Up to moderate acceptor concentration, it is found that fixing the donor and giving the acceptors a diffusion constant of $D=D_a+D_d$ introduces no measurable error into the calculation. This is an important result because it makes the analytical theory applicable to real systems. For high concentrations, at which acceptor–acceptor excluded volume becomes important, the static donor approximation introduces some error. In most systems of experimental interest, the static donor approximation is accurate.

In the theory that is discussed here and presented in more detail in Refs. 29 and 30, the ion population decays strictly by geminate recombination. This is because there is no other mode of ion decay built into the model. Within the context of the theory, an ion pair that becomes well separated will eventually recombine as $t\rightarrow\infty$. Therefore, there is no formal ''ion escape.'' In a real system, impurities or other chemical species mixed into the solution can act as scavengers and quench ions prior to geminate recombination. The theory described here can be used to gain insight into ion escape by recognizing that there is a separation of time scales for true geminate recombination versus formal $t\rightarrow\infty$ geminate recombination that is contained in the theory. In the exponential form of the transfer rate, $R_b$ defines the distance scale on which back electron transfer will occur. Ions that survive on a time scale long compared to the time for the diffusive root-mean-squared displacement to be greater than a few $R_b$, say $3R_b$, should be considered to have undergone escape. While this is not a perfectly well-defined criterion, on the long time scale associated with large ion pair separation, the decay of the ion population is very slow. Therefore, an exact definition of the time or distance for escape is not necessary.

The theory presented here uses the simplest picture of molecules moving in a liquid. The liquid is a continuum, with the donor and acceptors initially randomly distributed. The molecular motions are simple diffusion. However, the theory has been set up to be able to readily encompass more detailed and physically realistic models of liquid structure and dynamics. Two physical features of liquids are particularly important to the electron transfer problem. The first is the structure of the liquid around the donor. The local structure is not a continuum, but has solvent shells. This results in a significant change in the local acceptor concentration and, therefore, on the rate of electron transfer. The second is hydrodynamic effects. When a donor and an acceptor approach, they do not undergo the type of diffusive motion associated with a continuum. Hydrodynamic effects also have a significant impact on the rate of electron transfer. These physical features of liquids are currently being included in the theory and will be the subject of a future publication.

## ACKNOWLEDGMENTS

This work was supported by the Department of Energy, Office of Basic Energy Sciences (Grant No. DE-FG03-

84ER13251). The computers used to perform the calculations were purchased through departmental equipment Grant No. NSF-CHE 9408185 from the National Science Foundation with matching contribution provided by Stanford University.

[1] D. N. Beratan, J. Am. Chem. Soc. **108**, 4321 (1986).
[2] P. Siders and R. A. Marcus, J. Am. Chem. Soc. **103**, 748 (1981).
[3] B. S. Brunschwig, S. Ehrenson, and N. Sutin, J. Am. Chem. Soc. **106**, 6858 (1984).
[4] N. R. Kestner, J. Logan, and J. Jortner, J. Phys. Chem. **78**, 2148 (1974).
[5] Y. J. Yan, M. Sparpaglione, and S. Mukamel, J. Phys. Chem. **92**, 4842 (1988).
[6] H. McConnell, J. Chem. Phys. **35**, 508 (1961).
[7] M. V. Smoluchowski, Z. Phys. Chem. Leipzig **92**, 129 (1918).
[8] N. Agmon and A. Szabo, J. Chem. Phys. **92**, 5270 (1990).
[9] R. A. Marcus, Annu. Rev. Phys. Chem. **15**, 155 (1964).
[10] J. R. Miller, J. V. Beitz, and R. K. Huddleston, J. Am. Chem. Soc. **106**, 5057 (1984).
[11] M. Inokuti and F. Hirayama, J. Chem. Phys. **43**, 1978 (1965).
[12] M. D. Fayer, L. Song, S. F. Swallen, R. C. Dorfman, and K. Weidemaier, in *Ultrafast Dynamics of Chemical Systems*, edited by J. D. Simon (Kluwer Academic, Amsterdam, 1994).
[13] S. Chandrasekhar, Rev. Mod. Phys. **15**, 1 (1943).
[14] F. C. Collins and G. E. Kimball, J. Colloid Sci. **4**, 425 (1949).
[15] M. Tachiya, J. Chem. Soc., Faraday Trans. II **75**, 271 (1979).
[16] A. I. Burshtein, Chem. Phys. Lett. **194**, 247 (1992).
[17] R. C. Dorfman, M. Tachiya, and M. D. Fayer, Chem. Phys. Lett. **179**, 152 (1991).
[18] M. M. Agrest, S. F. Kilin, M. M. Rikenglaz and I. M. Rozman, Opt. Spectrosc. **27**, 514 (1969).
[19] J. Kusba and B. Sipp, Chem. Phys. **124**, 223 (1988).
[20] B. Sipp and R. Voltz, J. Chem. Phys **79**, 434 (1983).
[21] B. Sipp and R. Voltz, J. Chem. Phys. **83**, 157 (1985).
[22] I. Z. Steinberg and E. Katchalski, J. Chem. Phys. **48**, 2404 (1968).
[23] R. C. Dorfman, Y. Lin, and M. D. Fayer, J. Phys. Chem. **93**, 6388 (1989).
[24] R. P. Domingue and M. D. Fayer, J. Chem. Phys **83**, 2242 (1985).
[25] R. K. Huddleston and J. R. Miller, J. Phys. Chem. **86**, 200 (1982).
[26] P. Siders, R. J. Cave, and R. A. Marcus, J. Chem. Phys. **81**, 5613 (1984).
[27] S. Strauch, G. McLendon, M. McGuire, and T. Guarr, J. Phys. Chem. **87**, 3579 (1983).
[28] Y. Lin, R. C. Dorfman, and M. D. Fayer, J. Chem. Phys. **90**, 159 (1989).
[29] L. Song, R. C. Dorfman, S. F. Swallen, and M. D. Fayer, J. Phys. Chem. **95**, 3454 (1991).
[30] L. Song, S. F. Swallen, R. C. Dorfman, K. Weidemaier, and M. D. Fayer, J. Phys. Chem. **97**, 1374 (1993).
[31] S. A. Rice, *Diffusion-Limited Reactions* (Elsevier, Amsterdam, 1985).
[32] J. Crank, *The Mathematics of Diffusion* (Oxford University, London, 1956).
[33] R. M. Noyes, in *Progress in Chemical Kinetics*, edited by G. Porter (Pergamon, New York, 1961).
[34] R. C. Dorfman, Y. Lin, and M. D. Fayer, J. Phys. Chem. **94**, 8007 (1990).
[35] S. F. Swallen, K. Weidemaier, and M. D. Fayer, J. Phys. Chem. **99**, 1856 (1995).
[36] R. A. Marcus and N. Sutin, Biochim. Biophys. Acta **811**, 265 (1985); S. Murata, S. Y. Matsuzaki, and M. Tachiya, J. Phys. Chem. **99**, 5354 (1995).
[37] T. Asahi, M. Ohkohchi, R. Matsusaka, N. Mataga, R. Ping Zhang, A. Osuka, and K. Maruyama, J. Am. Chem. Soc. **115**, 5665 (1993); J. Cortés, H. Heitele, and J. Jortner, J. Phys. Chem. **98**, 2527 (1994).
[38] J. M. Myhre, in *Markov Chains and Monte Carlo Calculations in Polymer Science*, edited by G. Lowry (Marcel Dekker, New York, 1970).
[39] E. Parzen, *Stochastic Processes* (Holden-Day, San Francisco, 1962).
[40] J. Kemeney and J. L. Snell, *Finite Markov Chains* (van Nostrand, Princeton, NJ, 1960).
[41] M. P. Allen and D. J. Tildesley, *Computer Simulation of Liquids* (Clarendon, Oxford, 1987).
[42] J. M. Haile, *Molecular Dynamics Simulation* (Wiley, New York, 1992).
[43] J. P. Valleau and S. G. Whittington, in *Statistical Mechanics*, edited by B. J. Berne (Plenum, New York, 1977).
[44] J. P. Hansen and I. R. McDonald, *Theory of Simple Liquids* (Academic, London, 1976).
[45] K. U. Finger, A. H. Marcus, and M. D. Fayer, J. Chem. Phys. **100**, 271 (1994).
[46] G. Marsaglia and A. Zaman, J. Appl. Prob. **1**, 1 (1991).
[47] F. James, Comput. Phys. Commun. **60**, 329 (1990).
[48] W. H. Press, B. P. Flannery, S. A. Teukolsky, and W. T. Vetterling, *Numerical Recipes in C* (Cambridge University, Cambridge, 1988).